Ultrathin Three-Dimensional Thermal Cloak

Hongyi Xu,[1] Xihang Shi,[1] Fei Gao,[1] Handong Sun,[1,2,*] and Baile Zhang[1,2,†]

[1]*Division of Physics and Applied Physics, School of Physical and Mathematical Sciences, Nanyang Technological University, 21 Nanyang Link, Singapore 637371, Singapore*

[2]*Centre for Disruptive Photonic Technologies, Nanyang Technological University, 21 Nanyang Link, Singapore 637371, Singapore*

(Received 22 July 2013; published 3 February 2014)

We report the first experimental realization of a three-dimensional thermal cloak shielding an air bubble in a bulk metal without disturbing the external conductive thermal flux. The cloak is made of a thin layer of homogeneous and isotropic material with specially designed three-dimensional manufacturing. The cloak's thickness is 100 μm while the cloaked air bubble has a diameter of 1 cm, achieving the ratio between dimensions of the cloak and the cloaked object 2 orders smaller than previous thermal cloaks, which were mainly realized in a two-dimensional geometry. This work can find applications in novel thermal devices in the three-dimensional physical space.

DOI: 10.1103/PhysRevLett.112.054301 PACS numbers: 44.10.+i

An invisibility cloak [1–4] that can hide a three-dimensional (3D) object without disturbing external physical fields must possess a 3D geometry itself. A variety of cloaks working for different physical fields such as electromagnetic fields [5–16], acoustic wave fields [17,18] and elastic wave fields [19] have been experimentally demonstrated predominantly in a two-dimensional (2D) geometry, where the perceivable visibility in the third dimension was generally ignored. Implementing a 3D cloak to hide a 3D object is widely acknowledged as being extremely difficult in terms of fabrication and characterization. For example, significant efforts have been made to extend a cloak for electromagnetic waves from 2D to 3D by rotating [10] or extending [11] an original 2D design [20] to fill up the 3D space. However, due to the imperfection of the original 2D design [21], these 3D cloaks are still detectable in principle.

While the majority of cloaking research in the past few years focused on various wave fields, recently diffuse-field cloaks [14–16,22–24] are attracting more and more attention. A typical example is the thermal cloak that can hide objects from diffusive heat by guiding conductive thermal flux smoothly around a hidden object [25]. Most already reported demonstrations of thermal cloaks were based on transformation thermodynamics [26] (the heat diffusion equation is transformed with a coordinate transformation similar to previous transformation optics) that utilized artificial thermal metamaterials implemented mainly in the 2D geometry [22–24]. A 3D thermal cloak that can hide a 3D object in a thermal environment still remains unrealized. On the other hand, diffusion has distinct properties compared to wave, especially when the diffusion reaches equilibrium and does not change phenomenally. This can be utilized to facilitate the implementation of diffuse-field cloaks. For example, Ref. [15] utilized only commercially available materials to implement a cloak for static magnetic fields without applying coordinate transformation, but adopted a scattering cancellation method similar to previous plasmonic cloaking [2,9], because at extremely low frequencies the wavelength approaches infinity and local fields behave like diffuse fields reaching the steady state. This ingenious idea apparently will lead to remarkable fundamental breakthrough in cloaking research and significant applications in other relevant research fields that require guiding the diffusive field or energy flux.

Here we move one step forward to extend the 2D geometry in Ref. [15] to three dimensions by transferring the analysis into heat diffusion, and we demonstrate the first successful realization of a 3D thermal cloak working in the 3D space (see Supplemental Material for a movie documenting the functional thermal cloak in operation [27]). Recent preprints have shown the feasibility of this analysis transfer from static magnetic field to heat diffusion in both three [28] and two dimensions [29]. We choose an air bubble as the object to be cloaked, since it is well known that stationary air is a poor conductor of heat which approximates to a heat insulator in many cases, and small air gaps can seriously block the channel for heat exchange and cause local overheating—the main reason of thermal failure in mechanical and electronic devices. It is worth mentioning that what allows us to successfully fabricate a 3D cloak is a specially designed 3D machining process that is introduced for the first time in thermal cloaking research; we will elaborate on that process later. Another unique aspect of our 3D cloak is its ultrathin thickness, which allows the cloak to perform satisfactorily even in transient and inhomogeneous temperature fields. To the best of our knowledge, our demonstration is the only one so far that provides cloaking evidence for both the transient and the inhomogeneous temperature fields in 3D space.

For clarity purposes, we first briefly introduce the analysis transferred from Ref. [15] originally for static magnetic field yet applied here in heat diffusion. We start with the

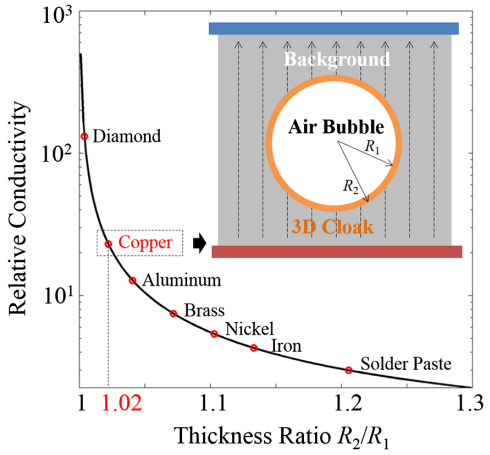

FIG. 1 (color online). Material candidates to realize a 3D thermal cloak with the background medium of stainless steel. The black curve shows the relative thermal conductivity required to implement a 3D thermal cloak with different thickness ratio of the cloak. The inset illustrates the cross section of the cloak (not to scale). Red or blue region denotes high or low temperature, and dashed arrows represent heat flux.

physical model of a spherical thermal cloak shielding a spherical air bubble in homogeneous conductive heat flux in thermal equilibrium, as illustrated in the inset of Fig. 1. The air bubble, in approximation to a heat insulator with thermal conductivity $\kappa_1 = 0$, locates at the center with radius R_1, being surrounded by a single-layer cloak with thermal conductivity κ_2 and outer radius R_2. Homogeneous heat flux diffuses from the bottom to the top through the background medium with thermal conductivity κ_b. The steady-state thermal diffusion equation in the homogeneous background takes the form $\nabla^2 T = 0$, where T is the temperature distribution in the homogeneous background. Temperatures of the air bubble T_1, of the cloak layer T_2, and of the background material T_b can be written down as

$$T_1 = -\sum_{l=0}^{\infty} A_l r^l P_l(\cos\theta) \quad (r \le R_1) \tag{1a}$$

$$T_2 = -\sum_{l=0}^{\infty} [B_l r^l + C_l r^{-(l+1)}] P_l(\cos\theta) \quad (R_1 < r \le R_2) \tag{1b}$$

$$T_b = -\sum_{l=0}^{\infty} [D_l r^l + E_l r^{-(l+1)}] P_l(\cos\theta) \quad (r > R_2), \tag{1c}$$

where $P_l(\cos\theta)$ is the lth order Legendre polynomials, A_l to D_l are constants to be determined, and (r, φ, θ) represent spherical coordinates. With the presence of the thermal cloak, the heat flux is expected to be undisturbed when passing by the air bubble. After solving Eq. (1) in a similar manner to Ref. [15], we can obtain the thermal conductivity κ_2 of the cloak as

$$\kappa_2 = \frac{\kappa_b(2R_2^3 + R_1^3)}{2(R_2^3 - R_1^3)}. \tag{2}$$

To fix the geometry, we plot the dependence of the relative conductivity of the cloak κ_2/κ_b on the thickness ratio R_2/R_1 in Fig. 1. We assume the background medium is stainless steel with thermal conductivity $\kappa_b = 15\,\mathrm{W/mK}$. The thermal conductivity of the cloak can be chosen from a variety of materials marked in red circles. Here we choose copper with thermal conductivity $\kappa_2 = 385$ W/mK to achieve a small thickness ratio R_2/R_1 at 1.02. Radii R_1 and R_2 are set to be 0.5 and 0.51 cm, respectively, meaning that a thin layer of copper with thickness of 100 μm is sufficient to cloak an air bubble with diameter of 1 cm. This ultrathin thickness of the cloak serves as a remarkable advantage to bypass the two intrinsic limitations of the above analytic design procedure. First, the above analytic design procedure, which was originally adopted in Ref. [15] to design a static magnetic cloak, is applicable only to homogeneous thermal flux, while inhomogeneous thermal flux will exhibit distortion around the cloak. However, as Ref. [15] shows, calculated in its Supplemental Material [27], a reduced thickness of the cloak can significantly reduce the distortion of the field from a pointlike diffuse source. Similarly, the ultrathin thickness selected here for the thermal cloak will allow the cloak to function satisfactorily in an inhomogeneous temperature field of a point heat source rather than being limited to homogeneous thermal flux. Second, the above analytic design procedure assumed the field has reached thermal equilibrium and thus is not applicable for a transient state. Note that previous designs for transient-state thermal cloaks [23,24] specifically concerned the product of density ρ and specific heat c of the cloak, essentially because it takes time to transfer heat to heat up the cloak (the product of density ρ and specific heat c represents the amount of heat required to heat up an unit volume of the cloak by an unit temperature increase) and it is difficult to synchronize the heating up processes of the cloak and the ambient medium. However, with an ultrathin thickness, i.e., a negligible volume, of the cloak, the heat transfer between the cloak and the ambient medium is almost instantaneous. Therefore, the synchronization of heating up the cloak and the ambient medium becomes automatic. Combined, these benefits allow the designed cloak to perform satisfactorily in both transient temperature field and inhomogeneous temperature field, as will be demonstrated in this Letter.

The specially designed 3D fabrication process is as follows. First, two blocks of stainless steel ASTM 301 with conductivity of 15 W/mK and dimension of $2 \times 2 \times 1$ cm were chosen as the background thermal medium where a temperature field can be present. In each block, a hemispherical hole with radius $R_2 = 0.51$ cm (precision less than 5 μm) was drilled with a precise electrical discharge machining where a series of rapidly recurring current discharges were applied to precisely erode the hole region in the steel block immersed in a dielectric insulating

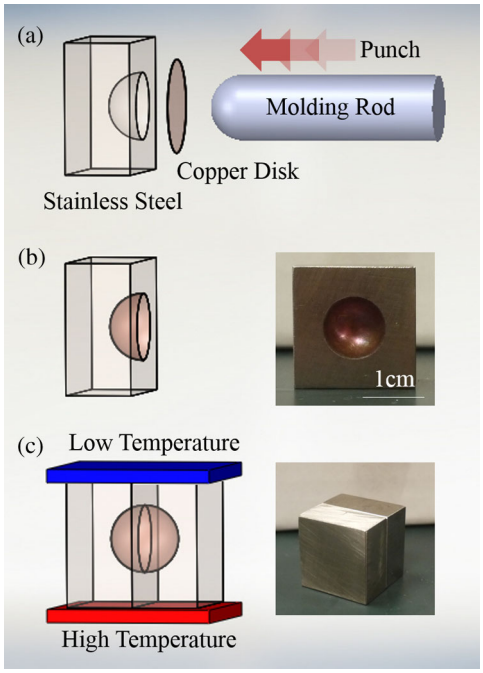

FIG. 2 (color online). Fabrication of a 3D thermal cloak. (a) Molding process of half of the 3D thermal cloak: a thin copper disk is punched into the hemispherical hole in the stainless steel block. (b) Illustration and snapshot of half of the thermal cloak after molding. (c) Illustration and snapshot of the full cloak by combining two half blocks. The red or blue plate represents high or low temperature at the bottom and top surface.

liquid. The surface roughness of the hemispherical hole was less than 1 μm. Second, copper with conductivity 385 W/mK was used to fabricate the single-layer cloak. Its excellent ductility is particularly suitable for the fabrication process shown in Fig. 2. As is shown in Fig. 2(a), a planar copper disk with thickness of 100 μm and surface area of 1.63 cm^2 (i.e., the surface area of the hemispherical hole in the stainless steel block) was aligned coaxially with the hemispherical hole. A molding rod with a hemispherical tip with radius of 0.5 cm was moved exactly above the hole covered by the copper disk. The molding rod then punched the copper disk with punching force around 300 N to press it conformably into the hemispherical hole. Because of the stress between the hemispherical hole in the steel block and the hemispherical tip of the molding rod, a copper shell [Fig. 2(b)] with homogeneous thickness was formed in the 100 μm gap between the hole and the tip. Note that during the process any air defect needs to be avoided to achieve a tight contact between the copper shell and the hole in the steel block. Besides, any misalignment among the hole, the copper disk, and the molding rod will also fail the whole manufacturing. Third, two identical half blocks with hemispherical copper shells punched into holes were combined to form a complete 3D cloak, as shown in Fig. 2(c). The dimension is 0.5 and 0.51 cm for the inner and outer radius of the copper spherical layer, and $2 \times 2 \times 2$ cm for the complete stainless steel block.

Now we proceed to demonstrate the effectiveness of the thermal cloak in transient homogeneous heat flux. As indicated in Fig. 2(c), the bottom surface and the top surface of the stainless steel block were attached to a hot plate (temperature 100 °C) and an ice tank made of aluminum (temperature 0 °C inside the tank), respectively, to create homogeneous heat flux diffusing from bottom to top. The bottom and top surfaces of the stainless steel block were coated with Coolermaster® thermal compound to enhance thermal contact with heat sources. It took a few minutes to reach thermal equilibrium for the whole system including the thermal contacts between the block and the ice container and between the block and the hot plate. The experiment was conducted in a sealed room to avoid ventilation. Note that the cloak is designed under the assumption that stationary air has almost zero thermal conductivity. Practically, stationary air has nonzero thermal conductivity of about 0.02 W/mK. Therefore the air bubble will be heated up. But the external temperature distribution in the ambient medium will not be affected significantly by this nonzero thermal conductivity of the air bubble.

To observe the temperature distribution inside the full steel block, we need to separate the two half blocks and measure the temperature distribution on the 2D cross section using an infrared (IR) camera FLIR® T640, which was calibrated with an Agema® laboratory blackbody. Because of the rotational symmetry of both the cloak and the temperature field, the full information of temperature distribution can be obtained by a simple rotation of the 2D image around its vertical axis. The reason we can separate the two blocks is because the thermal flux that diffuses from bottom to top does not cross the interface between the two half blocks. Moreover, as the ambient air is approximately a heat insulator, the heat transfer from the cross section of a half block to the ambient air does not significantly affect the temperature distribution in the half block. We have tested both the case of a separated half block being monitored all the time and the case of two half blocks being contacted for a while but separated just before the IR image was taken, and did not see an obvious difference. Technical challenges for measurement that did not appear in previous experiments of 2D thermal cloaks can be present here. Because the spherical cloak actually forms a volume cavity, some resonances of IR light inside the cavity will cause serious imaging artifacts. Moreover, the curved surface of the cloak with different depths will cause an out-of-focus effect for the IR camera. To correct the error caused by cavity resonances and the out-of-focus effect, and to exclude the emissivity influence from different materials, a 3M® Scotch Super 33+ vinyl electrical insulation tape with high emissivity of 0.95 and thickness around 140 μm was attached to the surface of a half block whose temperature was to be measured.

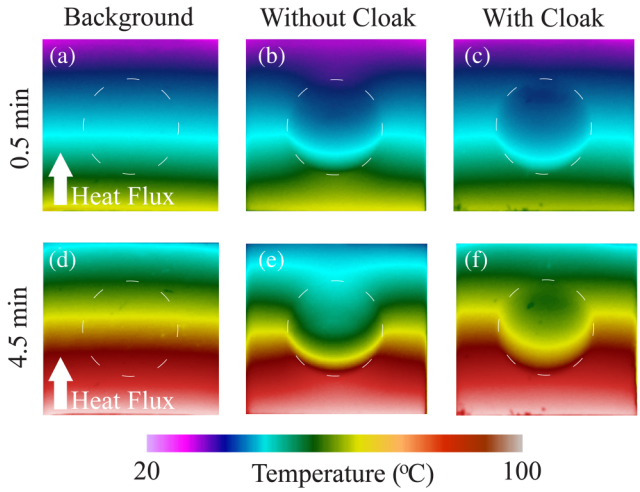

FIG. 3 (color online). Characterization of conductive thermal cloaking for transient homogeneous thermal flux. (a)–(c) Temperature distributions for the moment of 0.5 min in the beginning of heat transfer. (d)–(f) Temperature distributions for the moment of 4.5 min close to thermal equilibrium. (a) and (d) Temperature distributions in the pure background without any air bubble or cloak. (b) and (e) Temperature distributions when an air bubble is present without the cloak. (c) and (f) Temperature distributions when the air bubble is cloaked by the ultrathin cloak. In (b),(c) and (e),(f) the dotted circles indicate the position of the air bubble, while the dotted circles in (a) and (d) are merely for comparison.

The movie in the Supplemental Material [27] recorded the entire dynamic process in establishing the thermal equilibrium in the half block and the half cloak. We extract figures at two moments of 0.5 min (beginning of heat transfer) and 4.5 min (almost thermal equilibrium) for illustration in Fig. 3. It can be seen in Figs. 3(a) and 3(d) that, as time increases, the temperature field in the pure background (without the air bubble and the cloak) diffuses from bottom to top homogenously as expected. In Figs. 3(b) and 3(e), when there is an air bubble (without the cloak) embedded in the background medium, this air bubble seriously blocks the heat transfer, and cast a "shadow", or a relatively cool region, behind the air bubble. This kind of heat transfer blocking is detrimental to most heat exchange systems in which high efficient heat transfer is desired. In contrast, as shown in Figs. 3(c) and 3(f), when the cloak is in operation to shield the air bubble, the temperature in regions in front of and behind the air bubble has been clearly recovered when the heat flux passes by the air bubble, which means the air bubble no longer blocks the heat transfer from bottom to top. Admittedly, because the air bubble has nonzero thermal conductivity, the temperature inside the air bubble will increase slowly rather than staying unchanged. However, the raising speed of the temperature inside the cloaked air bubble is much slower than the corresponding positions in the background medium. Moreover, the thermal isolation of the cloak can be further improved by constructing double-layer highly reflective walls with vacuum in between

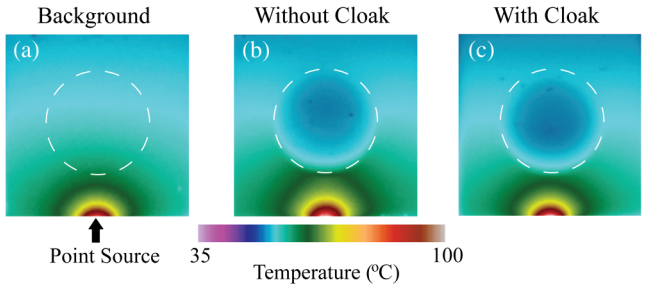

FIG. 4 (color online). Characterization of conductive thermal cloaking for an inhomogeneous temperature field from a point heat source. (a) Temperature distribution in the pure background without any air bubble or cloak. (b) Temperature distribution when an air bubble without the cloak is present close to the heat source. (c) Temperature distribution when the air bubble is cloaked by the ultrathin cloak. In (b),(c), the dotted circles indicate the position of the air bubble, while the dotted circle in (a) is merely for comparison.

(similar to a thermos bottle), but it will be out of the scope of this study.

To complete the characterization of this thermal cloak, we further demonstrate its cloaking performance in an inhomogeneous temperature field. Typically, we choose a point heat source to test the cloaking performance. Other inhomogeneous temperature profiles can be constructed by superposition of point heat sources. In the experiment, the bottom surface of the half steel block was touched by the tip of a soldering iron with temperature up to 450 °C, and the top surface of the half steel block was attached to the a hot plate with temperature of 40 °C. After the system reaches thermal equilibrium, the cross-section temperature distribution was captured by the IR camera. Figure 4(a) shows the temperature distribution in a pure background without the air bubble and the cloak. When an air bubble without the cloak is present, as shown in Fig. 4(b), the temperature below the air bubble is increased slightly because the air bubble blocks the heat diffuse from the point heat source at the bottom to the top surface. This heat blocking issue is relieved when the air bubble is surrounded by the cloak, as shown in Fig. 4(c), where the temperature distribution recovers to the situation in Fig. 4(a) when the air bubble does not exist.

In conclusion, we present the first realization of a 3D thermal cloak that can shield a spherical air bubble in a bulk metal from external conductive thermal flux. A special design with concepts transferred from the previously reported magnetic cloak is adopted without using thermal metamaterials and transformation thermodynamics. Novel 3D fabrication is for the first time introduced to fabricate diffuse-field cloaks. Experimental demonstrations are done for both transient and inhomogeneous temperature fields. The cloak can find wide cost-effective applications in addressing practical issues of heat transfer blocking in many relevant industries such as mechanical engine systems and semiconductor devices.

This work was sponsored by Nanyang Technological University under Grants No. M4080806.110 and No. M4081153.110, and the Singapore Ministry of Education under Grants No. M4011039.110 and No. MOE2011-T3-1-005.

Note added.—When our work was under consideration for publication, we found a recent independent publication reporting a bottom-up self-assembling method to optically cloak an aggregate of 3D nanospheres spread on a substrate [30]. Yet the main conclusions in our work are still valid.

*Corresponding author.
hdsun@ntu.edu.sg
†Corresponding author.
blzhang@ntu.edu.sg

[1] A. Greenleaf, M. Lassa, and G. Uhlmann, Physiol. Meas. **24**, 413 (2003).
[2] A. Alù and N. Engheta, Phys. Rev. E **72**, 016623 (2005).
[3] U. Leonhardt, Science **312**, 1777 (2006).
[4] J. B. Pendry, D. Schurig, and D. R. Smith, Science **312**, 1780 (2006).
[5] D. Schurig, J. J. Mock, B. J. Justice, S. A. Cummer, J. B. Pendry, A. F. Starr, and D. R. Smith, Science **314**, 977 (2006).
[6] R. Liu, C. Ji, J. J. Mock, J. Y. Chin, T. J. Cui, and D. R. Smith, Science **323**, 366 (2009).
[7] J. Valentine, J. Li, T. Zentgraf, G. Bartal, and X. Zhang, Nat. Mater. **8**, 568 (2009).
[8] L. H. Gabrielli, J. Cardenas, C. B. Poitras, and M. Lipson, Nat. Photonics **3**, 461 (2009).
[9] B. Edwards, A. Alù, M. G. Silveirinha, and N. Engheta, Phys. Rev. Lett. **103**, 153901 (2009).
[10] H. F. Ma and T. J. Cui, Nat. Commun. **1**, 21 (2010).
[11] T. Ergin, N. Stenger, P. Brenner, J. B. Pendry, and M. Wegener, Science **328**, 337 (2010).
[12] B. Zhang, Y. Luo, X. Liu, and G. Barbastathis, Phys. Rev. Lett. **106**, 033901 (2011).
[13] X. Chen, Y. Luo, J. Zhang, K. Jiang, J. B. Pendry, and S. Zhang, Nat. Commun. **2**, 176 (2011).
[14] S. Narayana and Y. Sato, Adv. Mater. **24**, 71 (2012).
[15] F. Gömöry, M. Solovyov, J. Šouc, C. Navau, J. Prat-Camps, and A. Sanchez, Science **335**, 1466 (2012).
[16] F. Yang, Z. L. Mei, T. Y. Jin, and T. J. Cui, Phys. Rev. Lett. **109**, 053902 (2012).
[17] S. Zhang, C. Xia, and N. Fang, Phys. Rev. Lett. **106**, 024301 (2011).
[18] B.-I. Popa, L. Zigoneanu, and S. A. Cummer, Phys. Rev. Lett. **106**, 253901 (2011).
[19] M. Farhat, S. Guenneau, and S. Enoch, Phys. Rev. Lett. **103**, 024301 (2009).
[20] J. Li and J. B. Pendry, Phys. Rev. Lett. **101**, 203901 (2008).
[21] B. Zhang, T. Chan, and B.-I. Wu, Phys. Rev. Lett. **104**, 233903 (2010).
[22] S. Narayana and Y. Sato, Phys. Rev. Lett. **108**, 214303 (2012).
[23] R. Schittny, M. Kadic, S. Guenneau, and M. Wegener, Phys. Rev. Lett. **110**, 195901 (2013).
[24] Y. Ma, L. Lan, W. Jiang, F. Sun, and S. He, NPG Asia Mater. **5**, e73 (2013).
[25] U. Leonhardt, Nature (London) **498**, 440 (2013).
[26] S. Guenneau, C. Amra, and D. Veynante, Opt. Express **20**, 8207 (2012).
[27] See Supplemental Material at http://link.aps.org/supplemental/10.1103/PhysRevLett.112.054301 for a movie documenting the functional thermal cloak in operation in transient homogeneous thermal flux.
[28] H. Xu, X. Shi, F. Gao, H. D. Sun, and B. Zhang, arXiv:1306.6835.
[29] T. Han, X. Bai, J. T. L. Thong, B. Li, and C.-W. Qiu, following Letter, Phys. Rev. Lett. **112**, 054302 (2014).
[30] S. Mühlig, A. Cunningham, J. Dintinger, M. Farhat, S. B. Hasan, T. Scharf, T. Bürgi, F. Lederer, and C. Rockstuhl, Sci. Rep. **3**, 2328 (2013).